Condensation of sp^3-Bonded Boron Nitride through a Highly Nonequilibrium Fluid State

Shojiro Komatsu,*,† Keiji Kurashima,† Yoshiki Shimizu,‡ Yusuke Moriyoshi,§ Masaharu Shiratani,# and Katsuyuki Okada†

Advanced Materials laboratory, National Institute for Materials Science, 1-1 Namiki, Tsukuba, Ibaraki, 305-0044, Japan, National Institute for Advanced Industrial Science and Technology, Tsukuba Central1, Tsukuba, Ibaraki 305-8561, Japan, College of Engineering, Department of Materials Science, Hosei University, 3-7-2 Kajino-machi, Koganei, Tokyo 184-8584, Japan, and Department of Electronics, Graduate School of Information Science and Electrical Engineering, Kyushu University, Hakozaki, Fukuoka 812-8581, Japan

Received: August 16, 2003; In Final Form: November 7, 2003

Exceptionally highly crystalline sp^3-bonded boron nitride showing Kikuchi lines in transmission electron diffraction was formed by pulsed laser vaporization deposition assisted with synchronously pulsated reactive plasma. Transmission electron microscopic observations indicated that a fluid-state precursor material was generated by the high-power nanosecond laser at 193 nm. Other sp^2- and sp^3-hybridized nanostructures with exceptionally wide variations in density, reflecting the original large density fluctuations, suggested that the precursor material was formed in the vicinity of the thermodynamic critical point (CP). These results as well as the exceptionally fast growth rates indicated a new mode of crystal growth, namely, the direct condensation of nonequilibrium-phase crystals from the fluid state near the CP.

Introduction

Kondepudi and Prigogine[1] suggest that a true revolution in materials science is in progress by handling highly nonequilibrium and nonlinear thermodynamical states of matter, through which new self-organized states and/or new orders of matter can be realized. They cite laser processing of materials as an example in which we can escape the "tyranny of the equilibrium phase diagram." Our recent report on the growth of highly crystalline sp^3-bonded boron nitride (BN) with a 5H-polytipic form by pulsed laser deposition with the help of synchronously modulated reactive plasma[2] at 10 Torr belongs in this category. The dense phase of BN with covalent bonds of tetrahedral coordination should find its thermodynamically stable position in the high-temperature and high-pressure region in view of the equilibrium phase diagram.[3] This report includes the TEM (transmission electron microscope) indications that fluid-state precursor BN is formed at or above the thermodynamic critical point (CP) in our process, and we conclude that a new mode of crystal growth occurs, that is, the metastable-phase crystal condensation from the fluid-state precursor in the vicinity of the CP (supercritical fluid, SCF, may be included). The growth mechanism of the sp^3-bonded BN through the highly nonequilibrium fluid state was modeled with a two-dimensional nonlinear dynamical system, in which the role of the plasma to induce an autocatalytic growth reaction was taken into account.

Experimental Section

The method for the synthesis of the 5H-polytypic form of sp^3-bonded BN and its characterization were reported previously.[2] Gaseous (or fluid-state) precursors for the deposition of BN, whose details are exactly the target of our research, were generated by the pulsed laser vaporization of sintered sp^2-bonded hexagonal BN using an ArF excimer laser at 193 nm with about a 20 ns pulse duration. Each laser plume was hit down by a packet of another reactive plasma from above, which was generated by modulating inductively coupled radio frequency plasma of an Ar/(1% NH_3) gas mixture with a square wave signal; the ambient gas pressure was about 10 Torr. The modulation signal for the plasma at 20 Hz was synchronized with the excimer-laser trigger by employing an appropriate delay time so as to make the reactive plasma packet effectively collide with the laser plume. Growth or transformation of BN is supposed to proceed in the collision space. By interrupting the flow of the collided and mixed plasmas with rolls of stainless steel mesh, we trapped the powder product. Adjustment of the position of the mesh trap controlled the time-of-flight, and powder products with different crystallinities and sizes were obtained accordingly. TEM was performed with acceleration voltages of 100 kV and 300 kV for observations in the micrometer and nanometer dimensions, respectively. Determination of the lengths and angles in the TEM and TED (transmission electron diffraction) images was done on scanned images using the computer software Canvas 6 or 8 (Deneba Systems, Inc.), which provided 2 or 3 significant figures depending on the case.

Preliminary dynamical analysis of the reactive plasma packets using two photodiode probes, which were positioned apart along the plasma flow, indicated that they propagated at approximately a few 10 meters per second. The flight time allowed for the BN particles was therefore on the order of 10 ms at most between the BN target and the mesh trap (5−10 cm apart). From this we may reasonably conclude that each crystal growth was completed when trapped in the stainless steel mesh, which acted as a growth stopper at low temperatures (below a few hundred

* Corresponding author. E-mail: Komatsu.Shojiro@nims.go.jp.
† National Institute for Materials Science.
‡ National Institute for Advanced Industrial Science and Technology.
§ Hosei University.
# Kyushu University.

10.1021/jp0364452 CCC: $27.50
Published on Web 12/11/2003

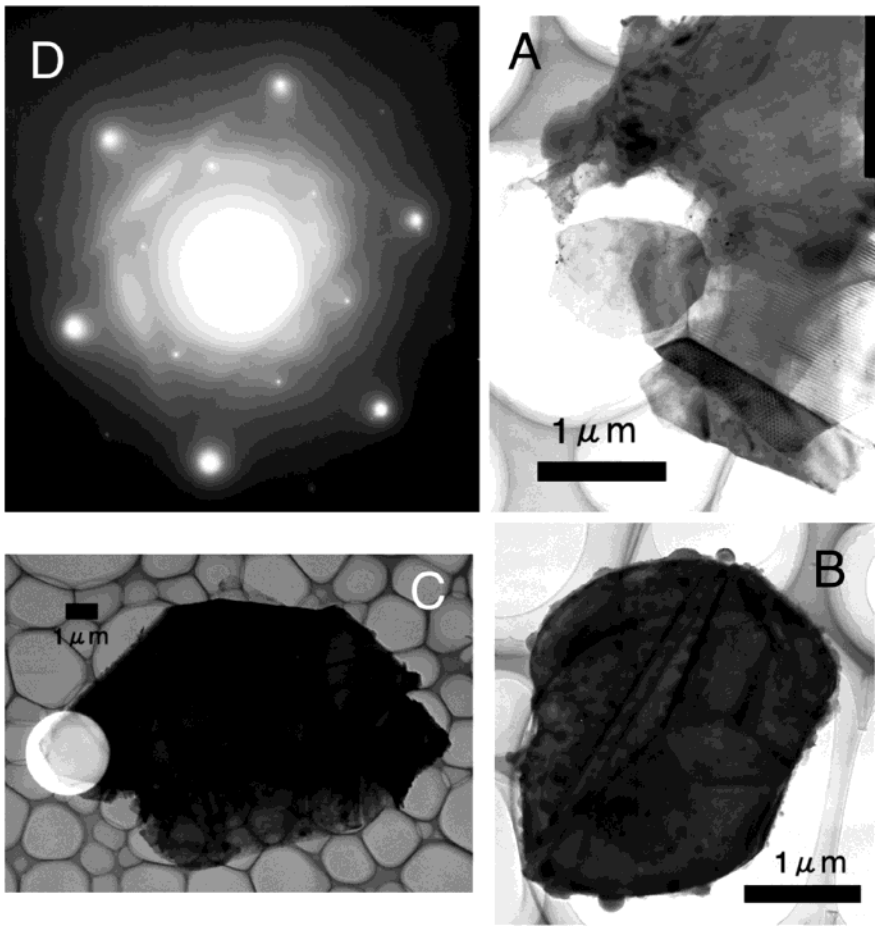

Figure 1. Growth of highly crystalline sp^3-bonded boron nitride (BN) with the 5H-polytypic form observed by TEM (A, B, and C) and TED (D). The Kikuchi lines of [0001] in D, which prove the excellent crystallinity of the sample, were obtained byTED analysis of the part indicated by a white disk in C. The corresponding high-resolution TEM of a microcrystallite is shown in Figure 2. Similar TEM images of these microcrystallites are also found in Figures 1 and 3 in ref 2.

°C) for each shot of the laser pulse at 20 Hz (within the repetition period of 50 ms). The exothermic growth processes have proceeded under the physical and/or chemical influences of the reactive plasma packets. The typical plasma density and the electron temperature measured with Langmuir probes were about 10^{14} cm^{-3} and 1 eV, respectively, for the plasma packets. It is noteworthy that mere laser ablation of BN in a vacuum with the same ablation conditions produced a barely observable quantity of deposit, while in the same reactive gas flow without plasma generation no sp^3-bonded BN was produced.

Results and Discussion

Highly Crystalline Microcrystallites of sp^3-Bonded BN. Two major categories of sp^3-bonded BN were found depending on the distance between the mesh trap and the BN target, *d*, which determined the time-of-flight of the precursor material or the rate for cooling of the "hot" precursor in the plasma. One category is highly crystalline sp^3-bonded 5H-BN crystallites of about 5−15 μm in diameter (Figure 1) obtained with a *d* value of about 10 cm. Another category is fine nanometer crystallites of sp^3-bonded BN embedded in a scarcely ordered matrix BN obtained with a *d* value of about 5 cm. The crystal structures of the micrometer crystallites were determined with TED and electron energy loss spectroscopy (EELS) as described previously.[2]

Incidentally, the original sp^3-bonded 5H-BN was prepared as film samples composed of 10 nanometer crystallites by chemical vapor deposition with the assistance of 193 nm laser irradiation of the growing film surface.[4] The stacking mode of the densely packed layers has a periodicity of 5 along the *c* axis in 5H-BN compared with 2 and 3 in the cubic and wurtzite forms, respectively. The film samples proved to have hexagonal lattice parameters *a* and *c* of 2.528 and 10.407 Å, respectively, by X-ray diffraction. The powder samples discussed in this report have proved to emit ultraviolet light at 225 nm (5.5 eV) by cathodeluminescence.[2]

Figure 1A shows agglomerated crystallites. The crystallites seen in Figure 1B,C have rather round shapes with the crystal edges seen through. In Figure 1C, the area irradiated by the electron beam of the TED instrument is indicated by a white disk. The corresponding TED pattern in Figure 1D indicates that the crystallite is sufficiently thick and perfect to give Kikuchi lines, which are of [0001] in this case.[5] The excellent crystallinity of the sample is also seen in the real lattice space in Figure 2, where the high-resolution TEM shows the crystal lattice of a microcrystallite in (0001); the unit cell of the sp^3-bonded 5H-BN is also drawn.

Nanocrystallites of sp^3-Bonded BN Embedded in a Scarcely Ordered Matrix. When *d* was set at 5 cm, the resultant products proved to be essentially nanocrystallites embedded in a scarcely ordered matrix (Figure 3A). These samples also showed similar EELS spectra as those shown previously,[2] principally due to the sp^3-bonded BN, though the resolution was in the micrometer range in this case. We could distinguish lattice images in the

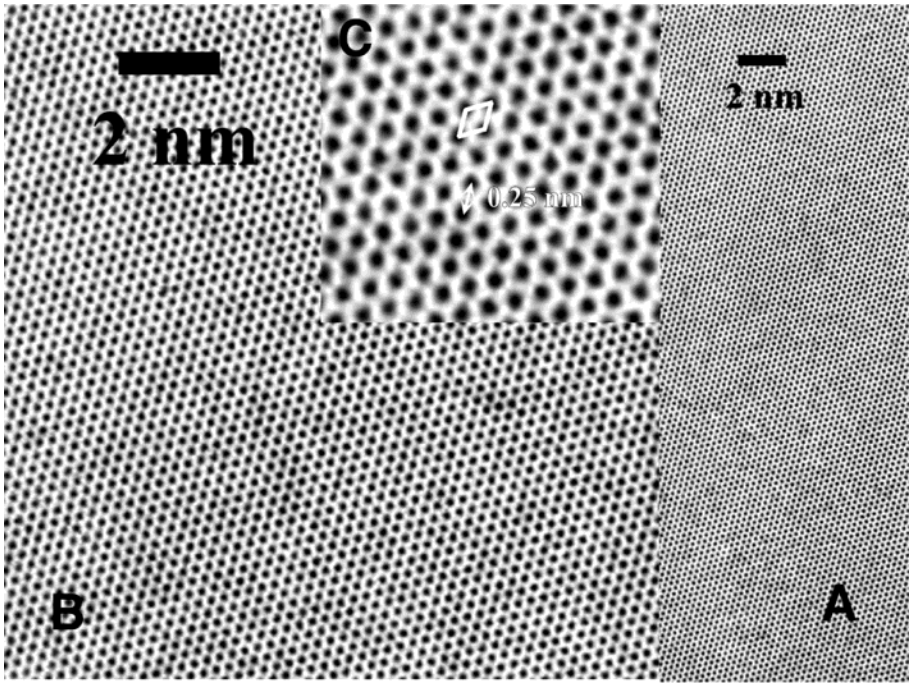

Figure 2. High-resolution TEM image of an sp^3-bonded 5H-BN microcrystallite with different enlargements. The lattice image on (0001) is seen. Few obvious crystal defects can be found by inspection, and this perfect crystallinity is consistent with the observation of the Kikuchi lines in Figure 1D, which also proves the high crystallinity in the reciprocal lattice. The hexagonal unit cell is drawn in C.

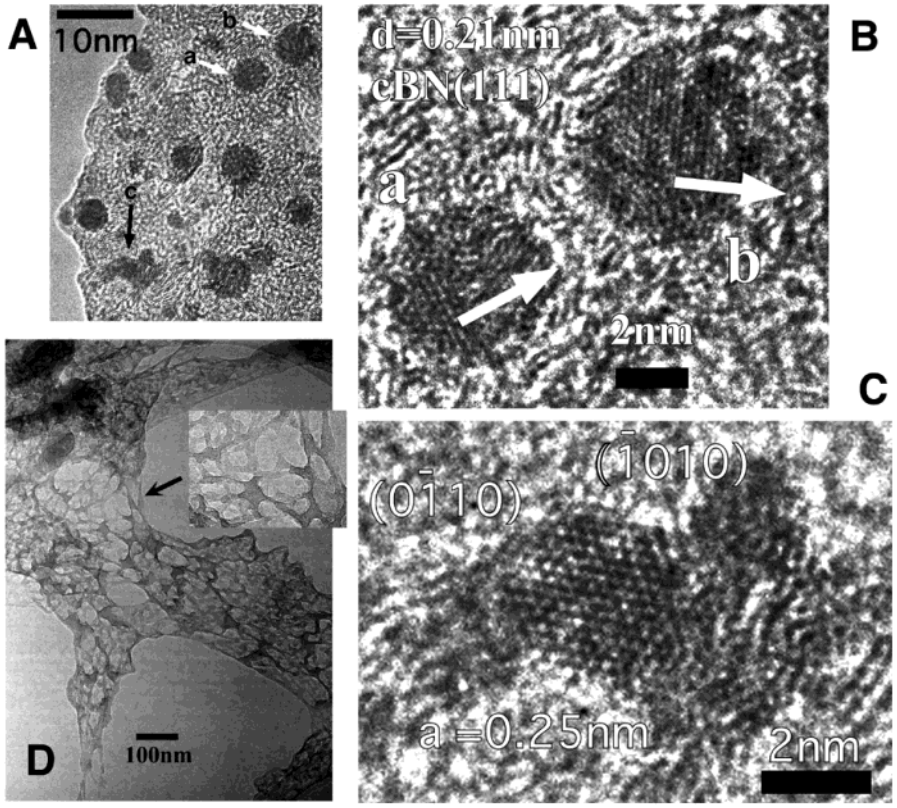

Figure 3. Growth of sp^3-bonded BN nanocrystallites embedded in a scarcely ordered matrix (A shows an overview, B and C show the enlargements), and a three-dimensional weblike structure obtained by rapid quenching of the precursor material generated by laser ablation of BN (D). We consider this strange structure shown in D to be reminiscent of the precursor BN in a fluid state before solidification, which was frozen without crystallization by rapid quenching.

dark nanoparticles as shown in Figure 3B (labeled a and b) and Figure 3C, which correspond to the particles a, b, and c in Figure 3A, respectively. In Figure 3B, interlayer spacings observed in the round particles a and b were 0.21 nm, which is in agreement with that for (111) in cubic BN (cBN).[6] The white arrows indicate the lattice vectors there. In Figure 3C, incomplete hexagonal morphology of a nanoparticle is found, in which the (−1010) and (0−110) crystallographic planes are indicated. The lattice parameter *a* of 0.25 nm, which was measured from the hexagonal arrangement of the lattice points, was in agreement

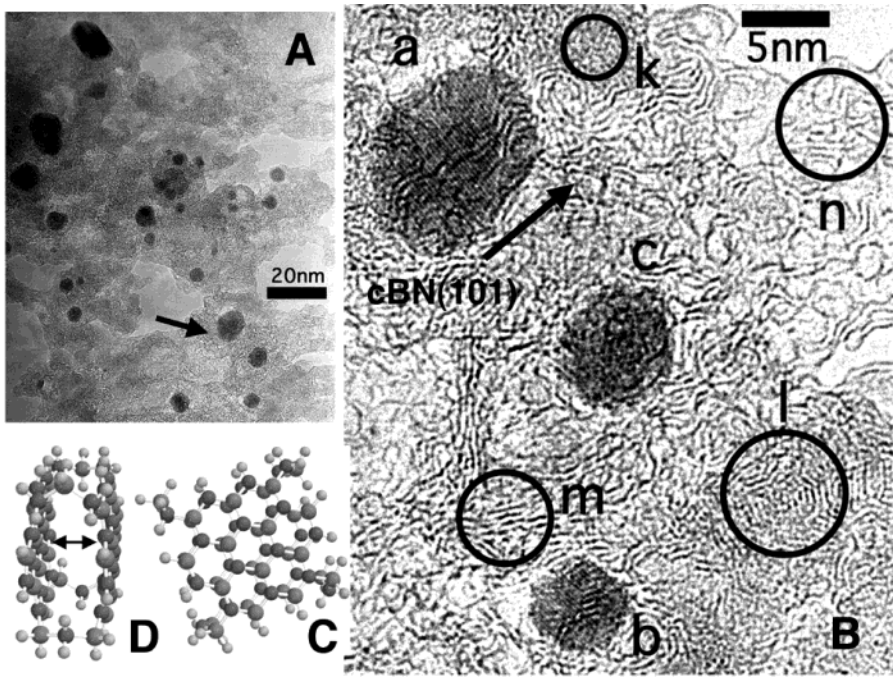

Figure 4. Growth of sp^3-bonded BN nanocrystallites embedded in a hardly ordered matrix with very large variations in density (A shows an overview, B shows the enlargement) that is considered to be reflecting the maximal density fluctuations of the precursor material in a fluid state near the thermodynamic critical point. Parts D and C show a structural unit made up of two sp^2-bonded BN platelets bridged by sp^3-bonded atoms at the four edges, which is modeled with the molecular orbital (MO) method; the half-dark and dark balls represent nitrogen and boron atoms, respectively, while the white balls denote hydrogen atoms that are introduced to facilitate the MO calculations by terminating the dangling bonds. These sorts of sp^2- and sp^3-hybridized units in various sizes, shapes, and stacking modes (thickness) are supposed to be major constituents in the complex structure of matrix BN.

with the sp^3-bonded 5H-BN.[4] We may understand that cBN nanoparticles tend to have round shapes due to their isotropic cubic symmetry while particles of sp^3-bonded 5H-BN tend to show hexagonal shapes reflecting the hexagonal symmetry. The image contrast between the nanoparticles and the matrix part is due to the difference in density. The matrix part has a lower density due to the hybrid structure composed of sp^3 and sp^2 bonds as will be discussed.

Precursor State for the Deposition. By interrupting the flight of the laser-induced plume by setting a silicon (100) substrate in contact with a water-cooled stainless steel holder a few centimeters above the BN target, we obtained a white powdery sample. Inspection of the sample by TEM revealed that it had a three-dimensional weblike structure with numerous 10−100 nm voids as shown in Figure 3D. It was very fragile under the electron-beam irradiation at the acceleration voltage of 300 kV. We consider this strange structure to be reminiscent of the precursor BN in a fluid state before solidification, which was "frozen" without crystallization by the rapid quenching.

The growth rate of 10 micrometer crystallites with perfect crystallinity within 10−100 ms as seen in Figure 1 is extraordinary faster[7] than that from the vapor phase, and we consequently have come to suppose that the direct condensation of fluid-state BN into the microstructured and nanostructured BN is very plausible.

Nanostructures with Exceptionally Wide Variation in Density. In Figure 4 other nanoparticles prepared under the same conditions as those used to prepare the sample presented in Figure 3 are shown. An overview of the dense nanoparticles embedded in the less-ordered matrix is seen in Figure 4A; the part indicated by an arrow is enlarged in Figure 4B. Particle a in Figure 4B shows lattice planes with an interlayer spacing of 0.25 nm, which is in agreement with cBN (101).[6] Particle b in Figure 4B also has a similar lattice image. We may consider the dark and rather round-shaped nanoparticles seen in Figure 4A to be mostly cBN nanoparticles.

On the other hand, the matrix part is neither homogeneous nor uniform as seen clearly in Figure 4B. For instance, the parts indicated by circles k, l, m, and n show variations in density. The almost complete loss of structural periodicity in the matrix is remarkable, and we understand that this structural complexity is not possible with only sp^2 bonding. All of the parallel planes that correspond to (0002) sheets in sp^2-bonded hexagonal BN (hBN) crystals[8] are finished with a very short period in subnanometer or nanometer dimensions. The interlayer distances show a wide range of variation, for example, from 0.38 nm (in part l) to 0.44 nm (in part n), which is larger than that of the bulk hBN (0002) value of 0.33 nm.[8] To make this point clearer, we performed a model simulation of the sp^2- and sp^3-hybridized structures of BN by using the semiempirical molecular orbital (MO) method at the PM3 approximation.[9] In this model, identical square-shaped platelets of sp^2-bonded BN (as seen in Figure 4C) are bridged by sp^3-bonded nitrogen and boron at the four edges (as seen in Figure 4D). In parts C and D of Figure 4, the half-dark and dark balls represent nitrogen and boron atoms, respectively, while the white balls represent hydrogen atoms, which were introduced to facilitate the MO calculations by terminating "dangling" bonds. The MO method at the PM3 approximation previously proved to be sufficiently reliable to model BN clusters.[10] The optimized interlayer distance in this model as indicated in Figure 4D, 0.42 nm, is in good agreement with observation. This model accordingly helps us to understand the origin of the enlarged interlayer spacings. These sorts of sp^2- and sp^3-hybridized units in various sizes, shapes, and stacking modes (thickness) are supposed to be major constituents in the complex structure of matrix BN. The ratio of sp^2 to sp^3 bonds appears to be increasing from part k to part n from this point of view in Figure 4B. It should also be noted that the

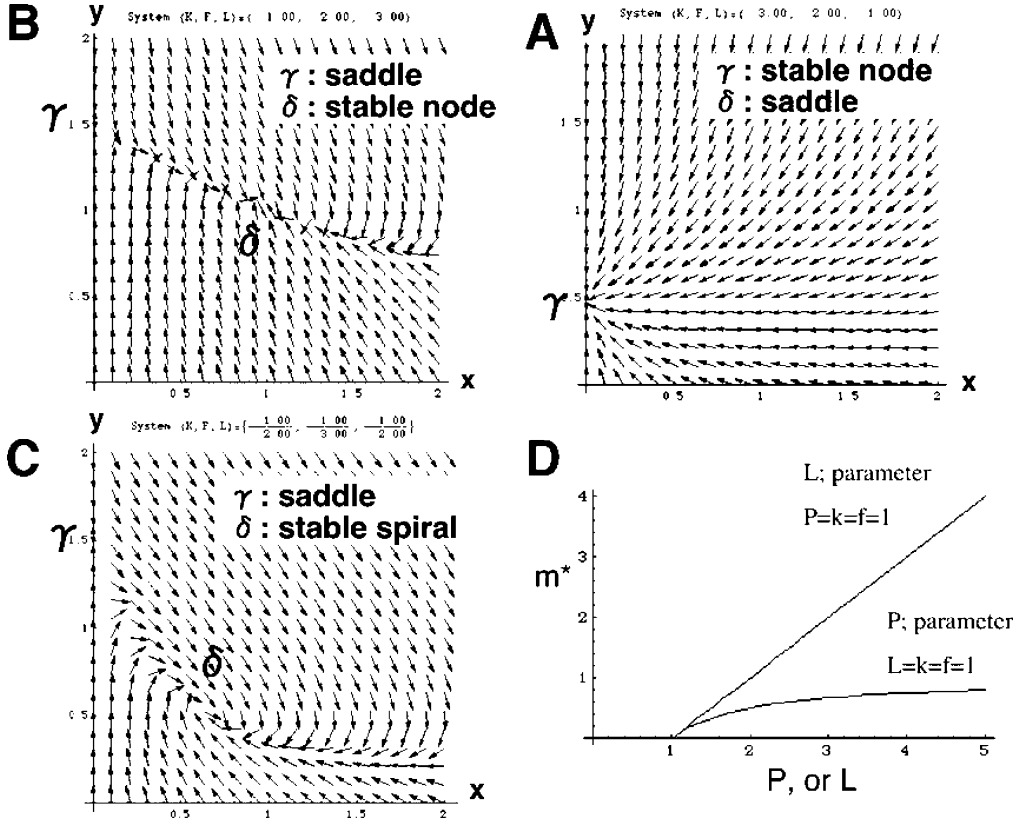

Figure 5. Vector field presentation for a two-dimensional nonlinear dynamical system which models the plasma-induced sp^3-bonded BN condensation from the fluid-state precursor. In the figure, $x = P^{1/2}m$ and $y = P^{1/2}M$, where P is the rate constant for the plasma-induced phase transition from precursor BN into purely sp^3-bonded BN, m is the quantity of purely sp^3-bonded BN, and M is the quantity of the precursor BN in the fluid state. In type A, point γ is a stable node, which means that we cannot expect the formation of sp^3-bonded BN. In types B and C, the two δ points are a stable node and a stable spiral, respectively, and there should be formation of sp^3-bonded BN. The expected quantity of the sp^3-bonded BN formation, namely, m^*, is plotted as a function of P and L in D, where L is the production rate of the precursor BN by laser ablation. We can find a threshold for the sp^3-bonded BN formation as a transcritical bifurcation phenomenon.

mere increase of the sp^3/sp^2 ratio should not ultimately lead to the formation of purely sp^3-bonded cBN or 5H-BN crystallites. We recognize here a discontinuity of the structural order or a phase transition. We also notice a qualitative difference between this sp^2- and sp^3-hybridized structure and a previously reported BN nanostructure,[11] which had little indication of an sp^3 component. We shed light on this point later by introducing a phase transformation model. It is also noteworthy that the hybrid crystal structure containing sp^2 and sp^3 bonded carbon, or "carbon foam", is theoretically predicted to be very stable and rigid.[12] The known structural similarity between carbon and BN[4] analogously leads us to expect the similar structural stability of sp^2- and sp^3-hybridized BN.

Nonlinear Dynamical System to Model the Plasma-Induced Autocatalytic Growth Reaction from the Fluid-State Precursor. To obtain a consistent view that explains the previous results, we propose a simple nonlinear model that is analogous to a model for laser action.[13] It was expected that an appropriate nonlinear dynamical model should reproduce the discontinuous structural transition observed previously.

Let $m(t)$ be the quantity of purely sp^3-bonded BN, $M(t)$ the quantity of the precursor BN in the fluid state, L the production rate of the precursor BN by laser ablation, P the rate constant for plasma-induced phase transition from precursor BN into purely sp^3-bonded BN, k the death rate of purely sp^3-bonded components (embryos), and f the rate at which the fluid precursor state transforms into solid phases other than the purely sp^3-bonded phase. These variables and constants are all not negative. Considering the gain and loss for the two independent variables $m(t)$ and $M(t)$, we introduce the following model

$$\frac{dm}{dt} = gain - loss = PmM - km \tag{1}$$

$$\frac{dM}{dt} = L - PmM - fM \tag{2}$$

The gain term PmM in eq 1 represents the production rate of purely sp^3-bonded components from the precursor BN, where the constant (or a parameter) P denotes the rate constant for a hypothetical plasma-induced autocatalytic reaction. It is known that autocatalytic reactions may lead to phase instabilities observed as bifurcation phenomena.[14] Introduction of this term reflects the experimental observation that plasma was necessary to produce sp^3-bonded BN. One of the roles of the plasma is evidently as a thermal absorber at appropriate temperatures for the exothermic growth reactions to proceed in the gas or fluid phase. For simplicity of modeling, we suppose here that the role of the nitrogen-related species generated from NH_3 was only to suppress the escape or separation of nitrogen from the BN precursor.

Let us introduce the following transformations to render the equations more understandable

$$x \equiv \sqrt{P}m, \quad y \equiv \sqrt{P}M, \quad \tau \equiv \sqrt{P}t$$
$$K \equiv k/\sqrt{P}, \quad F \equiv f/\sqrt{P} \tag{3}$$

Then the two-dimensional nonlinear differential equation system made of eqs 1 and 2 is simplified as follows

$$\frac{dx}{d\tau} = x(y - K) \equiv f(x, y) \tag{4}$$

$$\frac{dy}{d\tau} = L - (x + F)y \equiv g(x, y) \tag{5}$$

where x, y, K, F, and L are not negative. We find two fixed points γ and δ, where equilibrium states are realized, at $(0, L/F)$ and $(-F + L/K, K)$, respectively.

Stability analyses of the fixed points are carried out based on the linearization approximation of the nonlinear dynamical system, where eigenvalues of the Jacobians for the system give the criterions.[15] The results are summarized in Figure 5.[16] We find an exchange of stability between points γ and δ with the increase of LP as a parameter. When $LP < kf$, point γ is a stable node and point δ is a saddle (unstable). But point γ loses stability and becomes a saddle while point δ obtains stability as a stable node or a stable spiral under the condition $LP > kf$. A transcritical bifurcation is thus found to occur at the point $LP = kf$. This implies that we can expect the formation of purely sp^3-bonded BN only if the cooperation of the plasma and laser effects overcomes the product of the death rates of sp^3 embryos and the loss rate of precursor-state BN by non-sp^3 component formation. Under the condition $LP > kf$, the expected quantity of purely sp^3-bonded BN, m^*, is expressed as follows

$$m^* = -\frac{f}{\sqrt{P}} + \frac{L\sqrt{P}}{k} \tag{6}$$

The value of m^* is plotted in Figure 5D as a function of L or P. The straight line is for the case where $P = k = f = 1$ and L is taken as a parameter for the bifurcation, while the curve is for the case where $L = k = f = 1$ and P is taken as a parameter. Three types of stabilities for this dynamical system, namely, type A, type B, and type C, are drawn as vector fields in parts A, B, and C of Figure 5, respectively. Type A corresponds to the case in which $LP < kf$ and no sp^3 component is expected to form. In both types B and C we can expect the formation of sp^3 components, but the ways in which the phase points approach the fixed points are different. In type C, the temporal traces of the phase points have components of rotation (stable spiral), while they do not in type B (stable node). Detailed conditions for these further bifurcations are described in Figure 6. The implications of the difference between types B and C remain to be studied.

Condensation of Metastable-Phase Crystal from a Fluid State near the Thermodynamical Critical Point. The very wide range of density fluctuation observed in parts A and B of Figure 4 in the BN nanostructure has been seldom reported as far as the authors know. On the one hand, it is well-known that materials show the maximum density fluctuations at their thermodynamic critical point (CP).[17] It is accordingly tempting to consider these as "frozen" images or traces of BN in the fluid state near the CP. In the case of high-fluence nanosecond laser ablation of metals, "phase explosion", or the explosive decomposition of a superheated liquid phase into vapor and liquid phases at the spinode (the upper limit of the superheating), is known to proceed at the proximity of the CP (at around 0.9 Tc, where Tc is the critical temperature) accompanied by significant formation of droplets in the plume.[18] Explosive formation of droplets is frequently observed also in our experiments[19] with high laser fluence (at 50−100 J/cm^2), which is accordingly another indication that our experimental condition was near the CP. On the other hand, the fast growth of perfect crystals of minerals such as smectite has been known to proceed from the supercritical fluid (SCF) of water;[20] the SCF state has the property of high solubility of liquid water as well as the characteristic continuously variable density that may enable the fast and direct condensation of matter into the solid phase. We analogously suppose that a phase transition from the fluid-state of BN at the vicinity of the CP into the sp^3-bonded BN occurred here, in which the maximum fluctuation of density as well as that of the energy levels characteristic of the CP[21] favored the new type of phase formation.

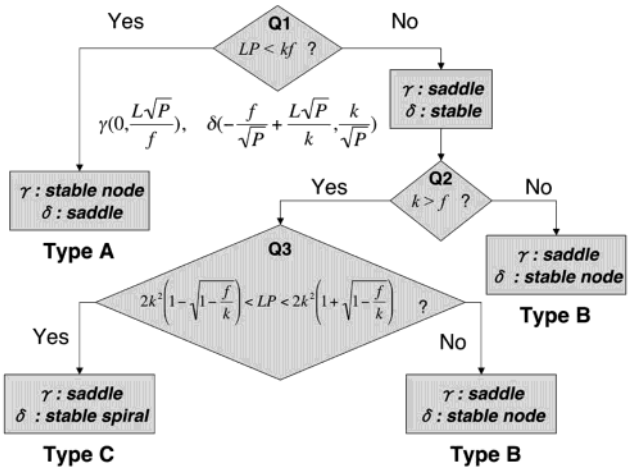

Figure 6. Block diagram presentation of the criterions for the stability analysis of the nonlinear dynamical system model. We find that a transcritical bifurcation takes place at $LP = kf$, where k is the death rate of purely sp^3-bonded components (embryos), and f is the rate at which the fluid-state precursor transforms into solid phases other than the purely sp^3-bonded phase. The criterion for the formation of sp^3-bonded BN in this model is thus $LP > kf$.

Acknowledgment. The authors are grateful for the kind and helpful advice from professor Toshiki Nakano at the National Defense Academy in Japan for the photoprobe measurements of the flow rate of the plasma.

References and Notes

(1) Kondepudi, Dilip; Prigogine, I. *Modern Thermodynamics: From Heat Engines to Dissipative Structures*; Wiley: New York, 1998; pp 459−460.
(2) Komatsu, S.; et al. *Appl. Phys. Lett.* **2002**, *81*, 4547.
(3) Bundy, F. P.; Wentorf, R. H., Jr. *J. Chem. Phys.* **1963**, *38*, 1144.
(4) Komatsu, S.; Okada, K.; Shimizu, Y.; Moriyoshi, Y. *J. Phys. Chem. B* **1999**, *103*, 3289.
(5) Loretto, M. H.; Smallman, R. E. In *Electron Microscopy and Microanalysis of Crystalline Materials*; Belk, J. A., Ed.; Applied Science Publishers: London, 1979; pp 59−66.
(6) Powder Diffraction File Card No. 35-1365; JCPDS-International Centre for Diffraction Data: Newton Square, PA, 1988.
(7) A simple estimation using the Hertz−Knudsen equation for molecular flux at a pressure of 10 Torr and temperatures of 1000−10 000 K predicts that the vapor growth within a few seconds should be negligibly small.
(8) Powder Diffraction File Card No. 34-0421; JCPDS-International Centre for Diffraction Data: Newton Square, PA, 1988.
(9) Stewart, J. J. P. *J. Comput.-Aided Mol. Des.* **1990**, *4*, 1.
(10) Komatsu, S.; Yarbrough, W.; Moriyoshi, Y. *J. Appl. Phys.* **1997**, *81*, 7798.
(11) Komatsu, S.; Shimizu, Y.; Moriyoshi, Y.; Okada, K.; Mitomo, M. *J. Appl. Phys.* **2002**, *91*, 6181.
(12) Umemoto, K.; Saito, S.; Berber, S.; Tomanek, D. *Phys. Rev. B* **2001**, *64*, 193409.
(13) Strogatz, S. H. *Nonlinear Dynamics and Chaos: With Applications to Physics, Biology, Chemistry, and Engineering*; Perseus Publishing: Cambridge, MA, 1994; p 81.
(14) Reference 1; p 439.
(15) Guckenheimer, J.; Holms, P. *Nonlinear Oscillations, Dynamical Systems, and Bifurcations of Vector Fields*; Springer: New York, 1983; pp 12−16.

(16) The vector fields are drawn using DynPac, a dynamical system software subpackage for Mathematica. Clark, A., Jr. *DynPac*; University of Rochester: Rochester, NY, 2002.
(17) Callen, H. B. *Thermodynamics and an Introduction to Thermostatistics*, 2nd ed.; Wiley: New York, 1985; pp 429, 425.
(18) Xu, X. *Appl. Surf. Sci.* **2002**, *197*−*198*, 61.
(19) Komatsu, S.; Shimizu, Y.; Moriyoshi, Y.; Okada, K.; Mitomo, M. *Appl. Phys. Lett.* **2001**, *79*, 188.
(20) Nakazawa, H.; Yamada, H.; Fujita, T. *Appl. Clay Sci.* **1992**, *6*, 395.
(21) Reference 17; p 425.